Theme V – Models and Techniques for Analyzing Seismicity

Earthquake triggering caused by the external oscillation of stress/strain changes

Takaki Iwata

Institute of Statistical Mathematics, Tokyo, Japan

Contents

Abstract We often observe that earthquakes are triggered by the external oscillation of stress/strain, and typical causes of the oscillation are the earth tides and seismic waves of a large earthquake. As no clear physical models of these types of earthquake-triggering events have been developed, statistical approaches are used for detection and discussion of the triggering effects. This article presents a review of suggestive physical processes, common statistical techniques, and recent developments related to this issue.

1 Motivation

Two major components are responsible for oscillation of stress/strain in the solid earth: earth tides and seismic waves. Compared with the response of seismic activity to static stress changes (see *CORSSA article by Hainzl et al.*), the response to oscillation of stress/strain has not been studied in depth because the earthquake pattern for oscillation of stress/strain is not simple given the complexity of earthquake physics.

Several studies have revealed a significant correlation between the occurrence of earthquakes and the earth tides (i.e., tidal triggering) for regional and small earthquakes [e.g., *Klein* 1976; *Rydelek et al.* 1988; *Iwata and Nakanishi* 1998; *Wilcock* 2001; *Tolstoy et al.* 2002; *Stroup et al.* 2007; *Wilcock* 2009] and for global earthquakes [e.g., *Tsuruoka et al.* 1995; *Tanaka et al.* 2002a; *Cochran et al.* 2004; *Métivier et al.* 2009]. A strong correlation was also found for aftershock sequences [e.g., *Mohler* 1980; *Souriau et al.* 1982; *Iwata* 2002; *Crockett et al.* 2006]. Additionally, an investigation of non-volcanic tremors [*Obara* 2002] is currently underway, and tidal triggering for such events has been found [e.g., *Nakata et al.* 2008; *Thomas et al.* 2009].

The amplitudes of stress changes caused by earth tides are at most a few kPa (Fig. 1), which is much less than the typical stress drop for a large earthquake, which is thought to be on the order of $1 \sim 10$ MPa [e.g., *Ide and Beroza* 2001]. However, the rate of stress changes due to the earth tides is much greater than the rate of stress caused by tectonic loading, and it is reasonable to expect that seismic activity would show a significant correlation with earth tides.

In contrast to the observations and expectation described above, other studies have shown no clear evidence of tidal triggering [e.g., *Heaton* 1982; *Rydelek et al.* 1992; *Vidale et al.* 1998]. *Vidale et al.* (1998) suggested that the rate of stress increases from the ordinary tectonic loading in the nucleation process just before an earthquake, and it is much larger than the stress rate caused by earth tides. *Beeler and Lockner* (2003) conducted laboratory experiments on rock friction and attempted to explain the absence of tidal triggering from the result of the experiments and the original friction law. Investigation of tidal triggering is related to
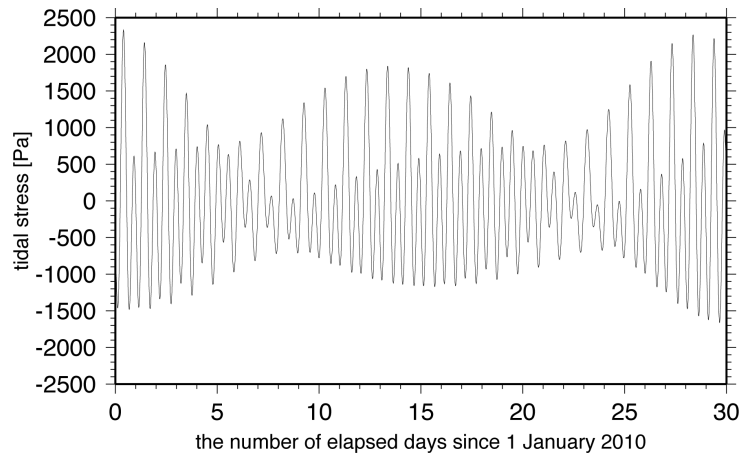
Fig. 1 Example of computed tidal normal horizontal stresses along the NS direction in the Tamba region, Japan (at 34.91°N, 139.05°E). The duration of the stresses was 30 days from 1 January 2010 (GMT), and SPOTL (Some Programs for Ocean-Tide Loading) was used in the computation.

the physics of earthquakes, and clarifying whether tidal triggering actually occurs would yield insight into the mechanics of earthquakes.

In some cases, a significant tidal triggering effect just before the occurrence of a great earthquake has been found [*Yin et al.* 1995, 2000; *Tanaka et al.* 2002b; *Zhang et al.* 2006; *Tanaka* 2010]. This implies that tidal triggering occurs when the state of stress is critical and suggests that the tidal triggering effect could be considered as a precursor to a great earthquake. Investigation of earthquake triggering will play an important role in earthquake forecasting, and this is another motivation to study tidal triggering.

As mentioned above, seismic waves also result in oscillation of stress/strain changes. On 28 June 1992, the Landers earthquake ($M_w = 7.3$) occurred in California, and earthquakes triggered by the transient stress changes due to the seismic waves of the Landers earthquake (i.e., dynamic triggering) were observed over a wide area [*Hill et al.* 1993]. Subsequent to these observations, dynamic triggering has been an area of active study [*Hill and Prejean* 2009 and references therein].

Studying only tidal triggering is insufficient to determine the responses of seismicity to oscillation of stress changes, because the ranges of periodicities and amplitudes of stress oscillation due to earth tides are limited. Seismic waves can cause larger amplitudes and shorter periods of stress changes than can earth tides. Therefore, it is necessary to study both of these earthquake-triggering phenomena to gain a complete understanding of the responses.

2 Starting Point

The following data are required to study the correlation between seismic activity and stress oscillations.

– Time series of an occurrence of earthquakes (i.e., an earthquake catalog).
– Focal mechanisms of triggered earthquakes and/or stress field of a studied region.
– Time history of stress/strain changes due to earth tides (for tidal triggering) or seismic waves (for dynamic triggering).

The Coulomb Failure Function (ΔCFF) plays an important role in earthquake triggering, and computing ΔCFF requires specifying the orientation of the fault planes of triggered earthquakes. Focal mechanisms and/or the stress field are informative for determining the orientation (see also *CORSSA article by Hainzl et al.*).

Occasionally, the time history of stress/strain changes can be obtained directly from measurements. However, if observational data are unavailable, the theoretical history is estimated by a computation. Theoretical strain changes caused by earth tides can be computed using the SPOTL (Some Programs for Ocean-Tide Loading) package [*Agnew* 1997], which is available for download without charge. *Tsuruoka et al.* (1995) (and references therein) discussed the theoretical background of the computation.

Normal-mode theory is frequently used in the computation of strain changes due to seismic waves. A detailed explanation of this theory was presented in Chapter 8 of *Aki and Richards* (2002).

No special statistical/seismological background is necessary to read this article. However, to achieve a deeper understanding of the discussion presented in Sect. 5.1.2, it is recommended that the reader consult the *CORSSA article by Zhuang et al.*

This article describes earthquake triggering caused by oscillation of stress/strain changes. However, another type of earthquake triggering is also associated with static stress changes. The *CORSSA article by Hainzl et al.* presented the physical and statistical aspects of static triggering, which are related to the topics discussed in this article.

3 Ending Point

By the end of this article, the reader will be aware of the following:

– The physical background/model of tidal and dynamic triggering.
– Some statistical approaches to modelling the triggered seismic activity.
– Examples of statistical studies on triggering phenomena.
– Remaining questions that should be addressed in future studies.

4 Physical Background

This section introduces two physical concepts to model the relationship between stress changes and seismicity rate. The style of the presentation borrows from *Kanamori and Brodsky* (2004), which describes the expected seismicity rate for constant stress rate with a stress step. Here a more general case is considered; a formulation of seismicity rate for arbitrarily stress changes is presented.

4.1 Rate- and state-dependent friction law

In the rate- and state-dependent friction law [*Dieterich* 1979; *Ruina* 1983], we assume that the frictional coefficient μ depends on slip speed $V = dt/dx$ and the state variable θ as follows:

$$\mu = \mu_0 + A \ln V + B \ln \theta, \tag{1}$$

and

$$\dot{\theta} = 1 - \frac{\theta V}{D_c}, \tag{2}$$

where μ_0 is the reference frictional coefficient, D_c is the critical slip distance, and A and B are constants.

If $|\theta V/D_c|$ is much greater than 1, we can approximate equation (2) as follows:

$$\dot{\theta} \approx -\frac{\theta V}{D_c}, \tag{3}$$

which is equivalent to

$$\theta = \theta_0 \exp(-x/D_c). \tag{4}$$

Then, equation (1) can be rewritten as

$$\mu = \mu_0 + A \ln V + B \ln \theta_0 - x/D_c. \tag{5}$$

If a temporal shear stress change $\tau(t)$ is imposed, the force balance is represented as follows:

$$\sigma(\mu_0 + A \ln V + B \ln \theta_0 - x/D_c) = -kx + \tau(t), \tag{6}$$

where k and σ are the stiffness of the material and normal stress, respectively.

We integrate equation (6) and obtain

$$x = -\frac{A}{H} \ln \left[-\frac{H}{A} e^{-\mu_0/A} \theta_0^{-B/A} \int_0^t e^{\tau(s)/A\sigma} ds + 1 \right] \tag{7}$$

and

$$V = -\frac{A}{H} \frac{-\frac{H}{A} e^{-\mu_0/A} \theta_0^{-B/A} e^{\tau(t)/A\sigma}}{-\frac{H}{A} e^{-\mu_0/A} \theta_0^{-B/A} \int_0^t e^{\tau(s)/A\sigma} ds + 1}, \tag{8}$$

where $H = -k/\sigma + B/D_c$. The slip speed V is infinitely large, and instability (i.e., an earthquake) occurs at $t = t_f$, which satisfies

$$\int_0^{t_f} e^{\tau(s)/A\sigma} ds = \frac{A}{H} e^{\mu_0/A} \theta_0^{B/A} = \frac{A}{HV_0} e^{\tau_0/A\sigma}, \tag{9}$$

where τ_0 and V_0 are shear stress and slip velocity at $t = 0$, respectively That is, this formula implies that an instability or earthquake occurs at $t = t_f$ if the slip $x = 0$ and the slip speed $V = V_0$ at $t = 0$.

We assume that the stress rate and the seismicity rate are constant. Hence, the stress as a function of time has the following form:

$$\tau = \tau_0 + \dot{\tau} t. \tag{10}$$

The constant seismicity rate is assumed to be $r_0 = 1/\Delta t$, where Δt corresponds to the time interval between the occurrences of two successive earthquakes. That is, the time of the occurrence of the n-th earthquake is given by

$$t_f = n\Delta t. \tag{11}$$

Substituting equations (10) and (11) into equation (9) yields

$$V_{0,n} = \frac{\dot{\tau} \left(e^{\dot{\tau} n \Delta t/A\sigma} - 1 \right)}{H\sigma}, \tag{12}$$

which is the slip speed of the n-th earthquake at $t = 0$ if the stress rate and seismicity rate are constant in time. Then, after substitution of $V_{0,n}$ in equation (12) into V_0 in equation (9), we solve the formula with respect to n:

$$n = \frac{A\sigma}{\dot{\tau}\Delta t} \ln \left[\frac{\dot{\tau}}{A\sigma} e^{-\tau_0/A\sigma} \int_0^{t_f} e^{\tau(s)/A\sigma} ds + 1 \right] \tag{13}$$

which shows that the n-th earthquake occurs at $t = t_f$ for stress change $\tau(t)$.

We rewrite t_f as t and compute the derivative with respect to t:

$$\begin{aligned} \frac{dn}{dt} &= \frac{1}{\Delta t} \frac{e^{(\tau(t)-\tau_0)/A\sigma}}{(\dot{\tau}/A\sigma) \int_0^t e^{(\tau(s)-\tau_0)/A\sigma} ds + 1} \\ &= r_0 \frac{e^{(\tau(t)-\tau_0)/A\sigma}}{(\dot{\tau}/A\sigma) \int_0^t e^{(\tau(s)-\tau_0)/A\sigma} ds + 1}. \end{aligned} \tag{14}$$

This formula represents the temporal seismicity rate change if the stress change $\tau(t)$ is given.

Based on this procedure, *Dieterich* (1994) proposed a model to derive the seismicity rate from the stress history based on the rate- and state-dependent friction of which details are described in the *CORSSA article by Hainzl et al. Dieterich* (2009) showed the expected time history of earthquake occurrences with stress oscillation. As shown in Fig. 10 of *Dieterich* (2009) the estimated seismicity rate increases with increasing stress, suggesting that most earthquakes occur near the stress peak. This study also showed that sufficiently large stress amplitudes ($> 3A\sigma$) are required to find a clear triggering effect.

In the derivation of the above formulas, the approximation of the original friction law is applied as shown in equation (3). Without using the approximation, it is difficult to show the relationships between $\tau(t)$ and t_f, n, and dn/dt in an analytical form. Without the approximation, however, these relationships can be obtained by numerical approaches such as the Runge-Kutta method [e.g., *Atkinson* 1989], and we can compute the response of seismicity to stress changes.

Some studies have conducted numerical simulations of dynamic triggering through the framework of the rate- and state-dependent friction law [*Gomberg et al.* 1997, 1998; *Belardinelli et al.* 2003]. These simulations included a linear increase in stress corresponding to tectonic loading and transient oscillation in stress changes mimicking seismic waves, and they computed the behavior of the spring-slider block.

These simulations suggested two hypotheses for triggering behaviour. The first is the "clock-advance" type, which suggests that dynamic stress changes hasten the occurrence of an earthquake. The time of instability of the block corresponding to an earthquake is sooner than that without transient oscillation (Fig. 2), and the instability does not always occur instantaneously at the time of oscillation. The duration of the delay or advance of the instability depends on the amplitudes, duration and period of the transient oscillation, parameters of the friction law, and condition of the system (time difference between the transient stress changes and original occurrence time of the instability if there are no transient stress changes).

In the second type of triggering behavior, dynamic stress changes generate "new" earthquakes, meaning that they would not have occurred without the stress changes. For a certain range of friction parameters, instead of instability of the block, a stable sliding corresponding to seismic creep occurs, such as in the San Andreas Fault [*Savage and Burford* 1973; *Thatcher* 1979] if only a linear increase of stress is imposed. In contrast, for the same range of parameters, instability can occur if a linear increase of stress and a transient stress change are both applied.
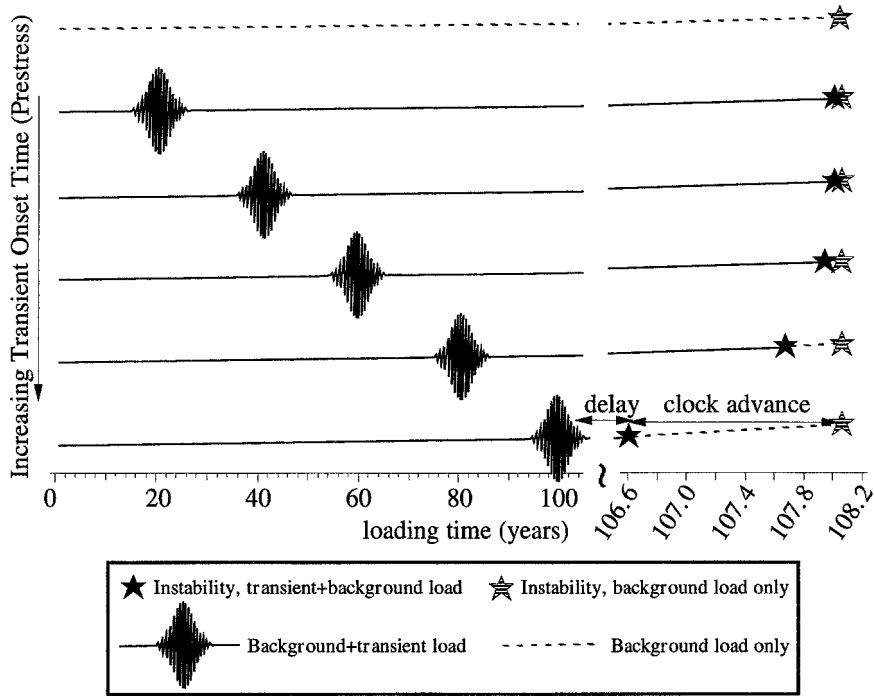
Fig. 2 Schematic diagram showing the behavior of a spring-slider block corresponding to "clock-advance". Instability of the block (i.e., an earthquake) would occur at the time denoted by grey stars if there were no transient stress changes corresponding to seismic waves. The transient stress changes hasten the occurrence of instability, as denoted by the solid stars. This figure is taken from *Gomberg et al.* (1997). (c) Seismological Society of America.

4.2 Stress corrosion

Another physical concept to describe the relationship between stress changes and seismicity is stress corrosion or sub-critical crack growth [e.g., *Atkinson* 1979].

Laboratory experiments indicated that the rate of growth of crack length x at time t is as described by [*Atkinson* 1979; *Das and Scholz* 1981]

$$V = \frac{dx}{dt} = V_0 \left(\frac{K}{K_0} \right)^p, \tag{15}$$

where p is the stress corrosion index, which is usually greater than ten and is related to the strength of the material. The parameter K is the stress intensity factor and has the following relationship with the crack length x and stress $\tau(t)$ [e.g., *Broberg* 1999]:

$$K = Y\tau(t)\sqrt{x}, \tag{16}$$

where Y is a constant and depends on the geometry of the crack. V_0 and K_0 are the rate of crack growth V and the value of the stress intensity factor K at $t = 0$,

respectively. Substitution of equation (16) into equation (15) and integration yields

$$x = x_0 \left(1 - \frac{p-2}{2} \frac{V_0}{x_0 \tau_0^p} \int_0^t [\tau(s)]^p ds \right)^{2/(2-p)}, \qquad (17)$$

and

$$V = \left(1 - \frac{p-2}{2} \frac{V_0}{x_0 \tau_0^p} \int_0^t [\tau(s)]^p ds \right)^{2/(2-p)} \frac{V_0}{\tau_0^p} [\tau(t)]^p, \qquad (18)$$

where x_0 and τ_0 are the crack length x and the stress $\tau(t)$ at $t = 0$, respectively.

In a similar manner as shown in Sect. 4.1, we derive the temporal seismicity rate change for temporal stress change $\tau(t)$. As p is normally larger than 10 and therefore $2/(2-p) < 0$, the rate of crack growth V is infinitely large at $t = t_f$ which agrees with the following condition:

$$\int_0^{t_f} [\tau(s)]^p ds = \frac{2}{p-2} \frac{x_0 \tau_0^p}{V_0}. \qquad (19)$$

To consider the case where stress rate and the seismicity rate are constant, we substitute equations (10) and (11) into equation (19) and obtain

$$V_{0,n} = \frac{2(p+1)}{p-2} \frac{x_0 \dot{\tau}}{\tau_0} \frac{1}{(1 + \dot{\tau} n \Delta t / \tau_0)^{p+1} - 1}. \qquad (20)$$

This shows the rate of crack growth of the n-th earthquake at $t = 0$ if the stress rate and the seismicity rate are constant.

We substitute $V_{0,n}$ in equation (20) into V_0 in equation (19) and obtain

$$\int_0^{t_f} [\tau(s)]^p ds = \frac{\tau_0^{p+1}}{\dot{\tau}(p+1)} \left[\left(1 + \frac{\dot{\tau} n \Delta t}{\tau_0} \right)^{p+1} - 1 \right]. \qquad (21)$$

Solving the above formula with respect to n yields,

$$n = \frac{\tau_0}{\dot{\tau} \Delta t} \left[\frac{\dot{\tau}(p+1)}{\tau_0^{p+1}} \int_0^{t_f} [\tau(s)]^p ds + 1 \right]^{1/(p+1)} - \frac{\tau_0}{\dot{\tau} \Delta t}, \qquad (22)$$

which shows that the occurrence time of the n-th earthquake is t_f if stress change $\tau(t)$ is applied.

We rewrite t_f as t and compute the derivative with respect to t:

$$\frac{dn}{dt} = r_0 \left[\frac{\dot{\tau}(p+1)}{\tau_0^{p+1}} \int_0^t [\tau(s)]^p ds + 1 \right]^{-p/(p+1)} \left[\frac{\tau(t)}{\tau_0} \right]^p, \qquad (23)$$

which shows the temporal seismicity rate change if the stress change $\tau(t)$ is given.

5 Available Statistical Methods

5.1 Methods of tidal triggering

5.1.1 Schuster's test

Schuster's test [*Schuster* 1897] is the traditional approach to investigate the periodicity of earthquakes. As shown in Fig. 1, the time history of the earth tides has complicated features, as it is a summation of several components with various time periods (approximately year, month, half month, day, and half day etc.). Therefore, we should choose which of these periodicities is to be examined, and convert the occurrence time of each earthquake to a phase angle relative to the earth tides. Fig. 3 shows how we make the conversion if focusing on the diurnal and semi-diurnal periodicity. The occurrence time t_i of the i-th earthquake is assigned to a phase angle linearly from -180° to 180°, where 0° corresponds to the local maximum of tidal stress to the occurrence time, and $-180°$ and 180° correspond to the local minima just before and just after the occurrence time, respectively. Then a statistic R is computed as follows:

$$R = \sqrt{\left(\sum_i^n \cos\theta_i\right)^2 + \left(\sum_i^n \sin\theta_i\right)^2}, \tag{24}$$

where θ_i and n indicate the phase angle of the i-th earthquake and the total number of examined earthquakes, respectively. If the probability distribution of θ_i is uniform, the computed statistic R represents the distance from the starting point of the walk in the two-dimensional random walk, which approximately follows the χ^2 distribution with 2 degrees of freedom. This approximation is appropriate if n is sufficiently large (> 10).

Hence, the probability p that the statistic is greater than or equal to R is given by

$$p = \exp\left(-\frac{R^2}{n}\right). \tag{25}$$

The above probability corresponds to the significance level required to reject the null hypothesis that the occurrence of the earthquakes has no periodicity with earth tides; a sufficiently small p-value (e.g., < 0.05) would suggest significant tidal triggering.

As shown in equation (25), Schuster's test is simple, and its statistic can be calculated with ease. This is the advantage of this test, but we also should note its disadvantage. The null hypothesis for Schuster's test assumes that all earthquakes occur independently. Hence, the existence of dependent or clustered earthquakes, such as aftershocks or swarms, leads to incorrect conclusions. To avoid such errors,
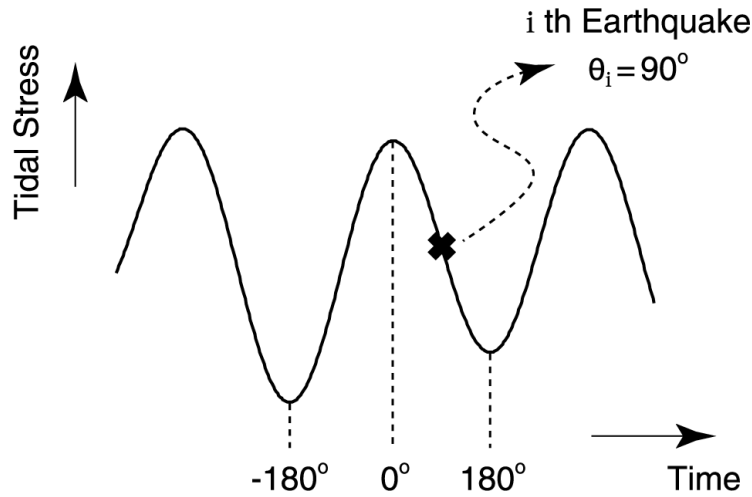
Fig. 3 Schematic diagram showing how to convert the occurrence time of an earthquake to the phase angle relative to the earth tides. This figure is taken from *Tanaka et al.* (2002a), and is produced/modified by permission of American Geophysical Union. Copyright 2002 American Geophysical Union.

it is necessary to remove clustered earthquakes before application of Schuster's test to the data, but it is complex to decluster a catalog (see the *CORSSA article by van Stiphout et al.*). Furthermore, declustering decreases the number of earthquakes, which reduces the power of detecting tidal triggering.

5.1.2 Point-process analysis

The point-process analysis (*CORSSA article by Zhuang et al.*) is another effective approach to investigate the periodicity of earthquakes. As shown in the previous section, the existence of clustered earthquakes is an obstacle in investigation of periodicity. To carry out the analysis without declustering, *Ogata* (1983) suggested using the sum of several components to express $\lambda(t)$ as follows:

$$\lambda(t) = \mu + (\text{trend}) + (\text{cluster}) + (\text{periodicity}), \qquad (26)$$

where $\lambda(t)$ represents an intensity function that corresponds to the expected number of events in a given unit time (e.g., the rate in one day) and is equivalent to the quantity dn/dt that appeared in equations (14) and (23) in Sect. 4. As this model considers clustered earthquakes and periodicity of seismicity simultaneously, it avoids the problems associated with catalog declustering.

To parameterize $\lambda(t)$, it is necessary to choose appropriate functional forms to represent the three components. For example, polynomial and trigonometric functions would be appropriate for the trend and periodicity components, respectively.

For the cluster component, *Ogata* (1983) originally suggested using the Laguerre-type polynomial to reduce the computation time [*Ogata and Akaike* 1982]:

$$\sum_{i=1}^{m} a_m t^{m-1} \exp(-ct). \tag{27}$$

However, modern computers allow the use of more complex functions derived from seismological considerations, such as the ETAS model [*Ogata* 1988; see also the *CORSSA article by Zhuang et al.*].

After the parameterization of the three components, we estimate parameters that provide the best fit to the observed time series of earthquakes by the maximum likelihood method. The log-likelihood ($\ln L$) for a point-process during the studied period $[S, T]$ is given by [e.g. *Daley and Vere-Jones* 2003]

$$\ln L = \sum_{i=1}^{n} \ln \lambda(t_i) - \int_{S}^{T} \lambda(t) dt. \tag{28}$$

We attempt to find the parameters that maximize the log-likelihood function.

To compare the goodness-of-fit of the cases where we do and do not assume the existence of tidal triggering, we apply the Akaike Information Criterion (AIC) [*Akaike* 1974]

$$\text{AIC} = -2(\text{maximum log-likelihood})$$
$$+ 2(\text{number of parameters}). \tag{29}$$

Cases with smaller AIC values are considered to show better fit to the observed time series of earthquakes.

As mentioned above, the point-process analysis has the advantage that it is not necessary to remove clustered earthquakes from a catalog. This approach also has other advantages over Schuster's test. Firstly, the point-process analysis allows simultaneous testing of different periodicities of tidal triggering, whereas they must be examined separately using Schuster's test. Secondly, temporal variation in tidal triggering effects can be examined smoothly through point-process analysis. To investigate the temporal variation by Schuster's test, earthquakes catalogs would have to be binned according to their occurrence times. In the binning process, it is necessary to ensure that all of bins include sufficiently large numbers of earthquakes, as the condition n should be satisfied for valid computation of the p-value in equation (25). Additionally results for binned data may depend on the length of the bins or time windows. The maximization of the log-likelihood function is often complicated but point-process analysis provides more objective results, as no binning process is required. An example showing the advantages will be described in Sect. 6.

5.2 Methods of dynamic triggering

Observations showing an abrupt increase in seismicity after the passage of seismic waves are candidates for dynamic triggering. To identify such candidates, it is necessary to compare the seismicity before and after the passage of seismic waves and to examine whether the increase is statistically significant. The β-statistic [*Matthews and Reasenberg* 1988; *Reasenberg and Matthews* 1988] is frequently used to compare seismicity rates in two time intervals, and has been applied for the detection of dynamic triggering in several studies [e.g., *Kilb et al.* 2000; *Gomberg et al.* 2001].

For n_1 and n_2 events during time periods 1 and 2 with time lengths t_1 and t_2, respectively, the β-statistic [*Matthews and Reasenberg* 1988; *Reasenberg and Matthews* 1988], which is used to determine whether the seismicity rate in period 2 is larger than that in the period 1, is given by

$$\beta = \frac{n_2 - n_1 t_2 / t_1}{\sqrt{n_1 t_2 / t_1}} \tag{30}$$

if the investigated sequence is assumed to follow a Poisson process. The β-statistic is expected to follow the standard normal distribution when the seismicity rates in the two periods are the same. Thus, from the computed β-statistic, we can determine the observed significance level to reject the null hypothesis that the two seismicity rates are the same. *Reasenberg and Simpson* (1992) regarded the difference between the two rates as significant if $|\beta| > 2$. In addition to the β-statistic, the statistics suggested by *Habermann* (1981) and *Marsan and Nalbant* (2005) can be used to identify significant seismicity rates changed (see the *CORSSA article by Marsan and Wyss*).

Behind the above statistics, we assume that an examined earthquake sequence follows a Poisson process. However, this assumption is often violated, as an earthquake sequence involves dependent earthquakes such as aftershocks and swarms. Therefore, a great deal of care is required in interpreting the computed β-statistic when using a non-declustered catalog. Instead of the β-statistic, *Harrington and Brodsky* (2006) used the empirical probability distribution of a number of earthquakes in each time bin over the period studied to compute the significance level. This approach is slightly more complicated, but it would be reasonable for a non-Poissonian sequence.

Another way to identify dynamic triggering involves focusing on the time interval between the arrival of seismic waves and the occurrence of the first subsequent earthquake. *Felzer and Brodsky* (2005) introduced the time ratio as follows:

$$R = \Delta t_2 / \Delta T, \tag{31}$$

where Δt_1 and Δt_2 represent the time intervals between the first earthquakes before and after the origin time T_M and ΔT is equal to $\Delta t_1 + \Delta t_2$ (Fig. 4). *Felzer and*
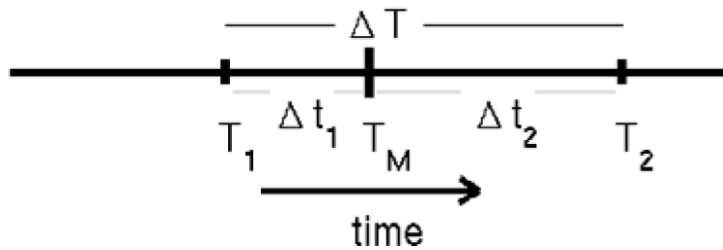
Fig. 4 Schematic diagram showing the definition of the time ratio R. This figure is taken from *Felzer and Brodsky* (2005), and is produced/modified by permission of American Geophysical Union. Copyright 2005 American Geophysical Union.

Brodsky (2005) used R to detect seismic quiescence, but *van der Elst and Brodsky* (2010) applied it to dynamic triggering. As R is expected to be 0.5 if events are distributed uniformly around T_M, earthquake triggering could be suggested if R is less than 0.5. Under a simple assumption regarding the occurrence of earthquakes (for instance, a Poisson process), the probability distribution of R can be derived analytically (see Appendix A of *van der Elst and Brodsky* (2010)), and hypothesis testing can be performed for dynamic triggering.

Additionally, *Iwata and Nakanishi* (2004) focused on the time interval between the arrival of seismic waves and the occurrence of the first subsequent earthquake. In their study, the observed distribution of the time intervals was compared with the expected distribution of the intervals generated by Monte Carlo simulation. If the observed distribution is significantly shifted to the left of the expected distribution, the shortened time interval represents evidence of dynamic triggering. This can be examined by the Kolmogorov-Smirnov test [e.g., *Gibbons* 1985].

6 Examples of Applications in the Literature

This section will present examples of the application of the methods introduced in the previous sections.

6.1 Application of Schuster's test for tidal triggering

Tsuruoka et al. (1995) divided the global earthquakes compiled in the Harvard centroid moment tensor (CMT) catalog according to their fault types and found evidence of tidal triggering only for normal faulting earthquakes. *Tanaka et al.* (2002a) followed the approach of *Tsuruoka et al.* (1995) but, using the more precise ocean-tide model and a larger data set taken from the CMT catalog than used in *Tsuruoka et al.* (1995), *Tanaka et al.* (2002a) demonstrated the strong tidal triggering for earthquakes with reverse or normal faulting.
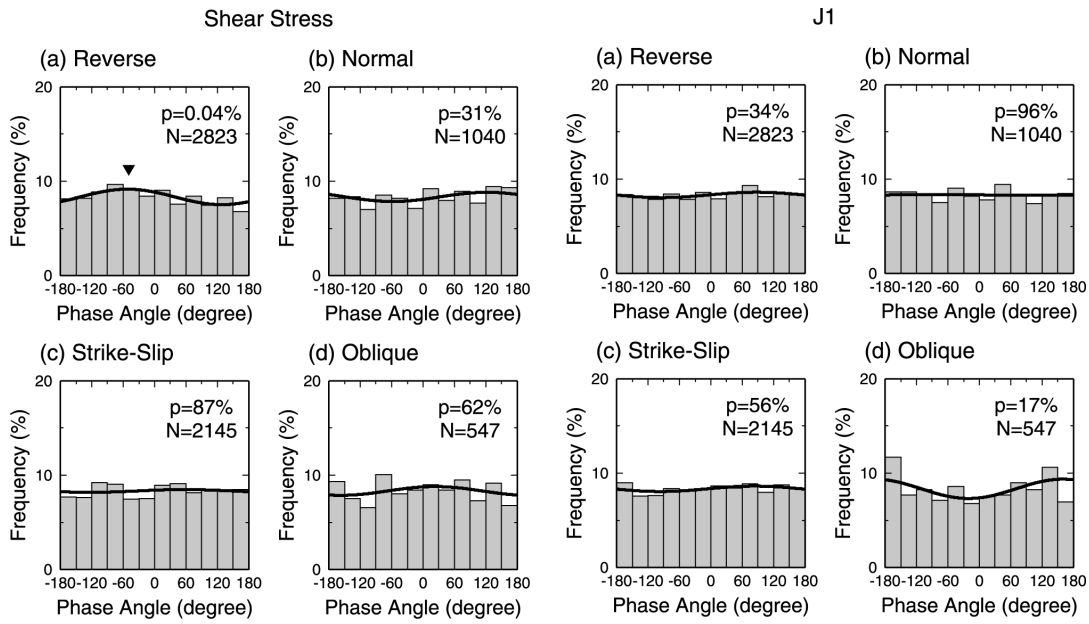
Fig. 5 Frequency distributions of the phase angles for earthquakes divided into four groups according to fault type. This figure is taken from *Tanaka et al.* (2002a), and is produced/modified by permission of American Geophysical Union. Copyright 2002 American Geophysical Union.

Tanaka et al. (2002b) investigated spatio-temporal variation in the tidal triggering effect in the Tonga-Kermadec region using a dataset based on the Harvard CMT catalog. The application of Schuster's method showed a significant correlation between the normal stress changes caused by the earth tides and the occurrence of earthquakes. To investigate temporal variation in the correlation, a window with a width of 1000 days was shifted by 50 days, and the p-values were computed for earthquakes included in each window. The results indicated that before the occurrence of the 1982 Tonga earthquake ($M_w = 7.5$), the p-value decreased as the endpoint of the time window approached the time point of the great earthquake occurrence, and the p-value did not indicate a significant effect after the large earthquake occurred (Fig. 6).

In a similar manner, *Tanaka et al.* (2002b) also investigated spatial variation in the tidal triggering effect by moving a window of 5° in increments of 1° in the north-south direction and computing the p-value for each window. As shown in Fig. 7, the p-value was significant only for the windows including the latitude of the Tonga earthquake.

In this approach, as mentioned in 5.1.2, we should note that the temporal or spatial variation of the significance may depend on the choice of the window size, and the dependency should be examined carefully. An idea to overcome this problem
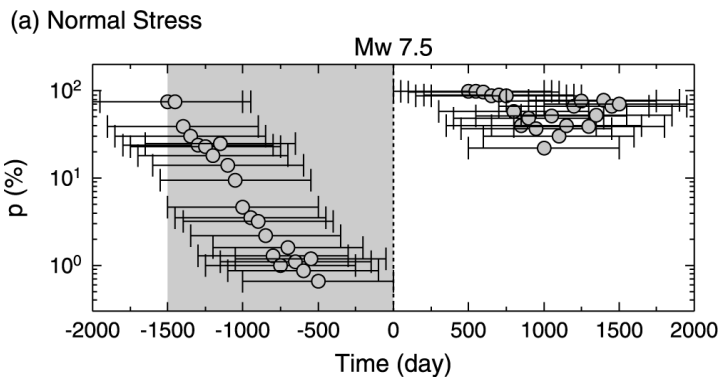
Fig. 6 Temporal variation in p-value for earthquakes in the Tonga-Kermadec region. The origin of the horizontal axis corresponds to the occurrence of the 1982 Tonga earthquake (19 December 1982), and the grey zone shows the period during which the p-value was significantly small ($< 5\%$). This figure is taken from *Tanaka et al.* (2002b), and is produced/modified by permission of American Geophysical Union. Copyright 2002 American Geophysical Union.
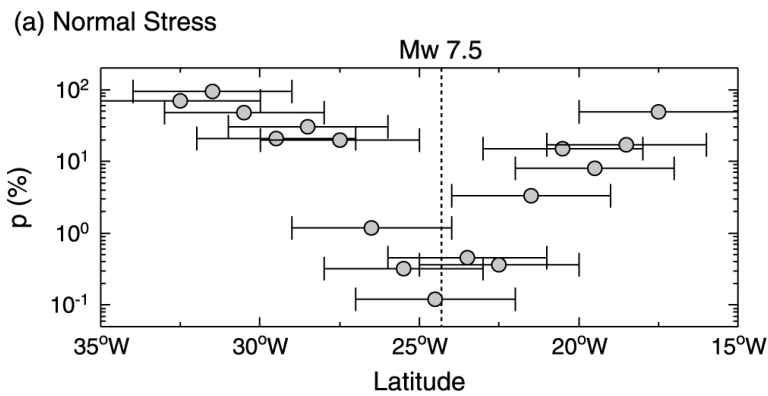

Fig. 7 Spatial variation in p-value for earthquakes that occurred during the 1500 days before the $M_w 7.5$ earthquake in the Tonga-Kermadec region. The vertical dotted line represents the latitude at which the large earthquake occurred. This figure is taken from *Tanaka et al.* (2002b), and is produced/modified by permission of American Geophysical Union. Copyright 2002 American Geophysical Union.

is to use a method without any predefined window, and the next subsection will introduce an example of such a method.

6.2 Application of point-process analysis for tidal triggering

Iwata and Katao (2006) applied point-process analysis to the tidal triggering by examining the correlation between the phase of the moon and the occurrence of microearthquakes (MEs) in the Tamba region, Japan. As mentioned in Sect. 5.1.2, this approach allows modelling of earthquake clusters and the periodicity of seismic activity simultaneously. Following equation (26), the following intensity function is

Constraints	(i)	(ii)	(iii)	(iv)
(N, L_1, L_2)	(3, 0, 0)	(3, 3, 0)	(3, 0, 3)	(3, 3, 3)
AIC	-4933.03	-4938.83	-4936.18	-4942.14

Table 1 Values of AIC, N, L_1, and L_2 obtained for the intensity function given by equation (33).

used:

$$\lambda(t) = \mu + \sum_{k=1}^{N} a_k t^k + \sum_{i;t_i<t} \frac{K \exp(\alpha(M_i - M_z))}{(t - t_i + c)^p}$$
$$+ A_1 \sin\theta(t) + B_1 \cos\theta(t) + A_2 \sin(2\theta(t)) + B_2 \cos(2\theta(t)), \qquad (32)$$

where $\theta(t)$ denotes the phase angle relative to the phase of the moon ($0°$ and $360°$ correspond to a new moon, and $180°$ corresponds to a full moon), and t_i and M_i are the occurrence time and magnitude of i-th ME, respectively. Note that we can investigate two periodicities of synodic and half-synodic months, as $\theta(t)$ and $2\theta(t)$ appeared in equation (32). The ETAS model [*Ogata* 1998] was used to represent clustered earthquakes.

Using the above intensity function, the following four cases were considered: (i) there is no triggering effect related to the phase of the moon; (ii) there is an effect that is only related to a synodic month; (iii) there is an effect that is only related to a half-synodic month; and (iv) there is an effect that is related to both synodic and half-synodic months. These can be expressed by the following constraints on the parameters in equation (32): (i) $A_1 = A_2 = B_1 = B_2 = 0$; (ii) $A_2 = B_2 = 0$; (iii) $A_1 = B_1 = 0$; and (iv) no constraint.

For each of the four cases, the best parameter values were computed by the maximum likelihood method, and then the comparison of the goodness-of-fit of these cases was conducted by AIC as described in Sect. 5.1.2. Note that the number of parameters N in the polynomial function representing trends was also determined using AIC. Consequently, the case (iv) was chosen as the best of the four cases.

To investigate temporal variation in the strength of the tidal correlation, the intensity function shown in equation (32) was modified as follows:

$$\lambda(t) = \mu + \sum_{k=1}^{N} a_k t^k + \sum_{i;t_i<t} \frac{K \exp(\alpha(M_i - M_z))}{(t - t_i + c)^p}$$
$$+ \sum_{k=1}^{L_1} A_{1k} t^{k-1} \cdot \sin\theta(t) + \sum_{k=1}^{L_1} B_{1k} t^{k-1} \cdot \cos\theta(t)$$
$$+ \sum_{k=1}^{L_2} A_{2k} t^{k-1} \cdot \sin(2\theta(t)) + \sum_{k=1}^{L_2} B_{2k} t^{k-1} \cdot \cos(2\theta(t)). \qquad (33)$$

As in the case with equation (32), the values for parameters N, L_1, and L_2 were determined by means of AIC. To investigate the periodicity associated with synodic and/or half-synodic months, four cases with constraints on L_1 and L_2 in equation (33) were examined: (i) $L_1 = L_2 = 0$; (ii) $L_1 \geq 0$ and $L_2 = 0$; (iii) $L_1 = 0$ and $L_2 \geq 1$; and (iv) $L_1 \geq$ and $L_2 \geq 1$.

The sequence of MEs occurring during the 4-year period following 17 January 1995 was also analyzed. Table 1 shows the AIC, N, L_1, and L_2 for the four constraints, suggesting that the triggering effects related to both synodic and half-synodic months are significant. Fig. 8(a) shows the estimated intensity functions representing the periodicity as a function of the number of days elapsed since 17 January 1995 and the phase angle, where 0° and 360° correspond to the time of new moon and 180° corresponds to a full moon. To clarify the temporal change of the strength in the triggering effect, the following function is computed:

$$g_i(t) = \sqrt{\left(\sum_{k=1}^{L_i} A_{ik} t^{k-1}\right)^2 + \left(\sum_{k=1}^{L_i} B_{ik} t^{k-1}\right)^2} \quad (i = 1, 2), \tag{34}$$

which shows the amplitudes of the intensity functions related to synodic or half-synodic months, and is plotted in Fig. 8(b).

The origin time of the study period was set as the time of 1995 Kobe earthquake, and the studied region is located next to the main fault of the great earthquake. The seismicity rate in the Tamba region increased compared with that before the Kobe earthquake, and this increase was suggested to be caused by a positive stress increase due to the main rupture of the Kobe earthquake [e.g., *Toda et al.* 1998]. As shown in Fig. 8(b), the strength of the tidal triggering effect was most remarkable immediately after the occurrence of the Kobe earthquake and then became gradually weaker over time. The tidal effect before the Kobe earthquake was also examined through the same approach, and it was not found to be significanct. These features suggest that the stress enhancement due to the Kobe earthquake produced the tidal triggering in the Tamba region.

6.3 Estimation of physical parameters on earthquake triggering

We derived the relationships between seismicity and physical parameters in Sects. 4.1 and 4.2. This implies that we can estimate the parameters from the observed earthquake sequence and stress history.

As mentioned in Sect. 4.1, *Dieterich* (1994) constructed a model to represent seismicity in response to changes in stress. *Nakata et al.* (2008) applied this model to the periodic activities of non-volcanic tremors observed in May 2005 and February 2006 in southwestern Japan. They assumed that the transient stress activated the
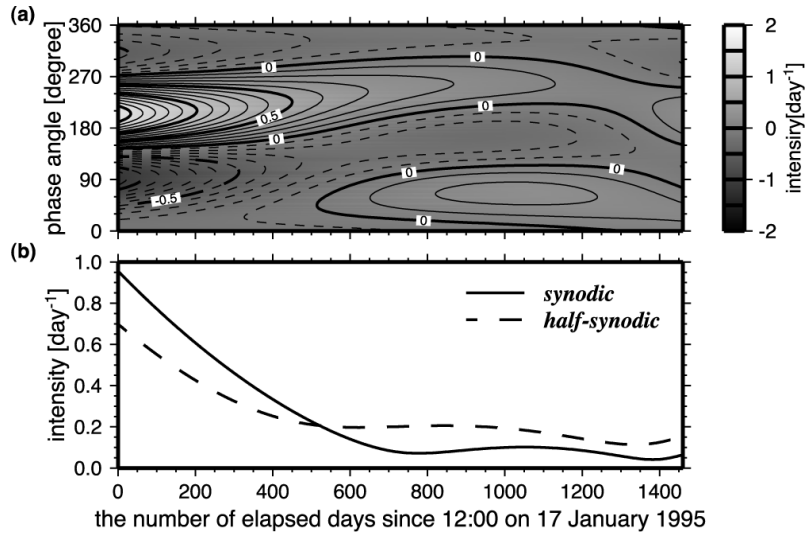
Fig. 8 (a) Temporal variation in the intensity functions of the trigonometric part in equation (33) obtained by analyses of microearthquakes during the 4-year period since 17 January 1995. (b) Temporal variations in $g_i(t)$ as shown in equation (34). The solid and dotted lines correspond to $g_i(t)$ related to synodic ($i = 1$) and half-synodic ($i = 2$) months, respectively. This figure is taken from *Iwata and Katao* (2006), and is produced/modified by permission of American Geophysical Union. Copyright 2006 American Geophysical Union.

tremor and that the earth tides caused the periodicity. A transient stress rate of $4 - 6$ kPa/day and $A\sigma$ of 1.3 kPa were estimated to optimize the fit of the tremor activity expected from the model with the observations.

If there is a stepwise stress increase in $\Delta\tau$, according to equations (14) and (23), the seismicity rate increases by a factor of $\exp[\Delta\tau/(A\sigma)]$ in the model of the rate- and state-friction law or $[1 + (\Delta\tau/\tau_0)]^p$ in the stress corrosion model. *Cochran et al.* (2004) assumed that the seismicity rate was not influenced by the previous stress history due to earth tides and was determined only by the present stress; i.e., the factors shown above. By fitting the factors with the frequency of global earthquakes as a function of stress amplitude due to the earth tides, they estimated $A\sigma = 64$ kPa for the rate- and state-friction law and $p = 15.7$ for stress corrosion.

6.4 Application of the β-statistic for dynamic triggering

As shown in Sect. 5.2, if a comparison between the seismicity before and that after the arrival of seismic waves shows a sufficiently large β-statistic value (e.g., > 2), the increase in seismicity is regarded as statistically significant. However, it is questionable to conclude that the observed increase is caused by dynamic triggering if a significant β-statistic is found in only one area, as the timing of the increase may coincide with that of the chance arrival of seismic waves. The observation of
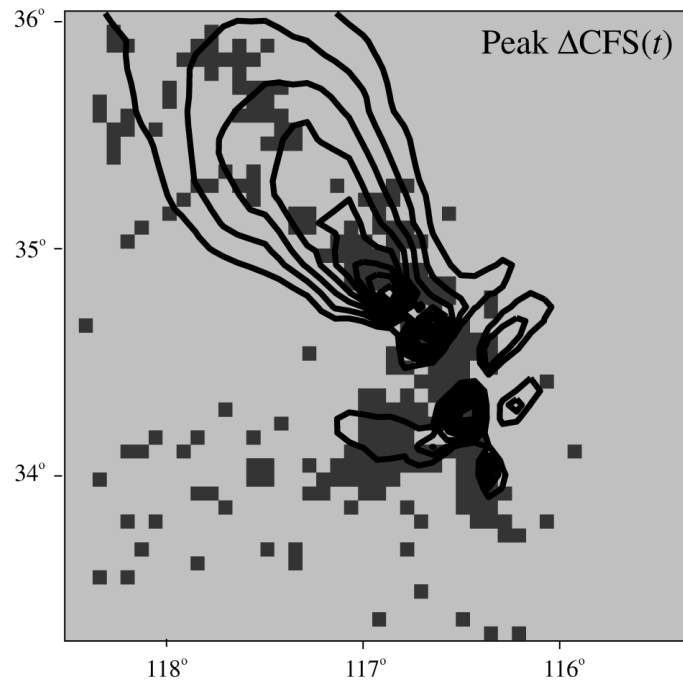
Fig. 9 Comparison between the spatial distributions of the β-statistic and peak amplitudes of stress changes due to seismic waves following the Landers earthquake. The contours represent the levels of the peak amplitude of stress changes exceeding 4 MPa with intervals of 1.5 MPa. The dark grey squares show the regions where the β-statistic is greater than 1. This figure is taken from *Kilb et al.* (2002), and is produced/modified by permission of American Geophysical Union. Copyright 2002 American Geophysical Union.

a clear increase in seismicity over a widespread area after the occurrence of a large earthquake would be evidence of dynamic triggering, and mapping the β-statistic is useful for identification of earthquake triggering.

The spatial pattern of the β-statistic provides insight into the mechanics of dynamic triggering. The spatial distributions of the β-statistic and peak amplitudes of stress changes due to seismic waves showed similar patterns in the aftershock regions of the Landers and Hector Mine earthquakes (Fig. 9) [*Gomberg et al.* 2001; *Kilb et al.* 2002; *Kilb* 2003]. The spatial pattern of dynamic stress changes showed a greater resemblance to that of increases in seismicity than that of static stress changes. These observations imply that dynamic triggering is more effective in the generation of aftershocks than is static triggering.

7 Summary, Further Reading, Next Steps

As discussed in the previous sections, suggestive physical theories and useful statistical methods have been proposed for studies of tidal/dynamic triggering, and the application of these methods has yielded useful information regarding these phe-

nomena. However, many fundamental problems remain to be resolved, as discussed below.

Physical process of dynamic triggering Some studies showed that the occurrence time of triggered earthquakes or low-frequency tremors agreed with the time of the largest amplitude of surface waves [e.g., *Prejean et al.* 2004] or the peak of stress/strain changes of the surface waves [e.g., *West et al.* 2005; *Miyazawa and Mori* 2006]. In contrast to these studies, the delay of dynamic triggering has frequently been reported [e.g., *Hill et al.* 1993].

The model based on friction law or stress corrosion can reproduce an abrupt increase in seismicity immediately after stress perturbation due to seismic waves but cannot explain the delay [*Gomberg et al.* 1998, 2001; *Belardinelli et al.* 2003]. Hence, other models are required for a comprehensive explanation of dynamic triggering.

Fluid dynamics in the crust may play an important role in dynamic triggering; for instance, changes of permeability [e.g., *Brodsky et al.* 2003], redistribution of pore pressure [e.g., *Hill et al.* 2002], and perturbation of the state of magma bodies [e.g., *Linde et al.* 1994]. For the above physical processes, a quantitative model describing the occurrence rate of triggered earthquakes has yet to be established, although this has been done for the friction law and stress corrosion.

Hence, to understand the physical process of dynamic triggering, the formulation of an earthquake sequence caused by fluid dynamics is required. Comparison between the expected and observed seismicity rates will allow discussion of detailed physical cause of dynamic triggering.

Clarification of the existence/non-existence of tidal triggering Several studies have indicated significant tidal triggering effects, as shown in Sect. 1, but there is still debate regarding the significance of these effects. Earthquakes can be classified into several groups depending on their occurrence time, location, fault type, magnitude, etc., and the observed significance levels for each of these groups are calculated to reject the null hypothesis that no tidal triggering occurred. In this case, it should be noted that the calculated significance levels are underestimated; a repetition of trials may show a "sufficiently small" significance level. The underestimation should be considered carefully to perform appropriate statistical evaluation (see also *Emter* (1997)).

We assume that shear stress or ΔCFF plays an essential role in earthquake triggering, and some physical models support this idea as discussed in Sect. 4. In general, studies of static and dynamic triggering investigate the relationship between seismicity and shear stress or ΔCFF. However, some studies of tidal triggering use other stress components, such as normal stress. The effects of stress components other than shear stress or ΔCFF in tidal triggering cannot be excluded, but these

components should be supported by physical concepts. Otherwise appropriate evaluation of the statistical significance will require focusing on the so-called multiple comparison problem in statistics.

Different types of earthquake triggering The studies introduced in Sect. 6.4 suggest that dynamic triggering plays a more important role in generating aftershocks than static triggering. However, this does not mean all aftershocks were caused by dynamic triggering; *Richards-Dinger et al.* (2010) discussed this point.

Probably the effects of static, dynamic, and tidal triggering simultaneously influence seismic activity. Hence, to deepen our understanding of the physics of earthquake triggering, it is important to use statistical approaches to separate the effects of the different type of earthquake triggering or to measure the fractions of the contribution given by the different triggering phenomena.

Computation of stress/strain changes A precise computation of stress/strain changes due to earth tides and seismic waves is essential, but such computation is still difficult. To study tidal triggering, it is necessary to take ocean tide loading into consideration [*Heaton* 1982; *Tsuruoka et al.* 1995]. *Tanaka et al.* (2002a) compared the computed strain changes based on the traditional ocean model of *Schwiderski* (1980) and a recent model proposed by *Matsumoto et al.* (2000), and showed that the introduction of the recent model significantly modified the computed strain changes. After this modification, however, some minor differences between the values obtained by computation and by observation remained. In the computation of strain changes due to seismic waves, the well-determined source model of the earthquake responsible for the seismic waves is necessary. The global CMT catalog provides one of the most reliable and useful point source models of global earthquakes, but the computed strain changes based on the global-CMT solutions and the normal mode theory are slightly different from the observed strain changes [e.g., *Nakanishi* 2005].

The ocean model and the CMT solutions probably have some errors. Such uncertainties should be taken into account in the computation of stress/strain oscillation. Additional uncertainties will arise from the complicated structure of the earth, the geometry of the faults of triggered earthquakes (i.e., receiver faults), the friction coefficient, etc. (see also the *CORSSA article by Hainzl et al.*)

These uncertainties should be minimiz ed as much as possible, but reduction of these uncertainties is difficult. Hence, in the computation of stress/strain oscillation, we should consider properly these uncertainties. For instance, *Hainzl et al.* (2009) used a Monte Carlo simulation for their computation of static stress changes, and this approach could be applicable to the computation of external stress/strain changes.

Impact on earthquake forecasting The studies introduced in Sect. 6 suggested that the tidal triggering effect is a precursor to a large earthquake. Therefore, the detection of the triggering effect may be attractive for earthquake forecasting.

To evaluate the efficiency of this approach, we have to know the frequency of significant tidal triggering, the percentage of tidal triggering that is not followed by great earthquakes, and the percentage of great earthquakes that are preceded by tidal triggering, etc. Only a few great earthquakes have been examined, but more comprehensive investigations will be necessary to address the above questions; thus, spatiotemporal variation in tidal triggering should be studied in detail with an earthquake catalog covering a wide area and a long time period.

It would also be of interest to determine the relationship between dynamic triggering and the next great earthquake. There have been no reports to date regarding such relationship, but this would also be an appealing area of study if triggering represents evidence of a near-critical stress state. By analogy to tidal triggering, further research regarding dynamic triggering is required. However, this is not an easy task, as many triggered earthquakes do not appear in earthquake catalogs. The existence of triggered earthquakes is frequently masked by large-amplitude seismic waves of a great earthquake, and they can be identified only after application of a high-pass filter to seismograms. Therefore, it is important to establish a tool to detect such masked earthquakes systematically.

Recommendations for further reading are as follows. Although written more than 10 years ago, *Emter* (1997) is still a good review of important works on tidal triggering over the last century. *Hill and Prejean* (2009)'s report is a valuable discussion of dynamic triggering. *Harris* (1998) and *Steacy et al.* (2005) presented comprehensive overviews of studies on tidal, dynamic, and static triggering of earthquakes, and these publications are useful references for determining areas of future research.

References

Agnew, D. C. (1997), NLOADF: A program for computing ocean-tide loading, *J. Geophys. Res.*, *102*, 5109–5110. 5

Akaike, H. (1974), A new look at the statistical model identification, *IEEE Trans. Automatic Control*, *AC-19*(6), 716–723. 13

Aki, K., and P. G. Richards (2002), *Quantitative Seismology (2nd ed.)*, University Science Books. 5

Atkinson, B. K. (1979), A fracture mechanics study of subcritical tensile cracking of cuartz in wet enviroments, *Pure Appl. Geophys.*, *117*, 1011–1024. 9

Atkinson, K. E. (1989), *An introcution to numerical analysis*, Wiley. 8

Beeler, N. M., and D. A. Lockner (2003), Why earthquakes correlate weakly with the soild Earth tides: Effects of periodic stress on the rate and probability of earthquake occurrence, *J. Geophys. Res.*, *108*, doi:10.1029/2001JB001518. 3

Belardinelli, M. E., A. Bizzarri, and M. Cocco (2003), Earthquake triggering by static and dynamic stress changes, *J. Geophys. Res.*, *108*, doi:10.1029/2002JB001779. 8, 22

Broberg, K. B. (1999), *Cracks and fracture*, Academic Press. 9

Brodsky, E. E., E. Roeloffs, D. Woodcock, I. Gall, and M. Manga (2003), A mechanism for sustained groundwater pressure changes induced by distant earthquakes, *J. Geophys. Res.*, *108*, doi:10.1029/2002JB002,321. 22

Cochran, E. S., J. E. Vidale, and S. Tanaka (2004), Earth tides can trigger shallow thrust falut earthquakes, *Science*, *306*, 1164–1166. 3, 20

Crockett, R. G. M., G. K. Gillmore, P. S. Phillips, A. R. Denman, and C. J. Groves-Kirkby (2006), Tidal synchronicity of the 26 December 2004 Sumatran earthquake and its aftershocks, *Geophys. Res. Lett.*, *33*, doi:10.1029/2006GL027074. 3

Daley, D. J., and D. Vere-Jones (2003), *An Introduction to the Theory of Point Processes*, vol. I, Springer, New York, USA. 13

Das, S., and C. H. Scholz (1981), Theory of time-dependent rupture in the earth, *J. Geophys. Res.*, *86*, 6039–6051. 9

Dieterich, J. (1994), A constitutive law for rate of earthquake production and its application to earthquake clustering, *J. Geophys. Res.*, *99*, 2601–2618. 8, 19

Dieterich, J. H. (1979), Modeling of rock friction, 1, experimental results and constitutive equations, *J. Geophys. Res.*, *84*, 2169–2175. 6

Dieterich, J. H. (2009), Application of rate- and state-dependent friction to models of fault slip and earthquake occurrence, in *Earthquake Seismology*, edited by H. Kanamori, pp. 107–129, Elsevier. 8

Emter, D. (1997), Tidal triggering of earthquakes and volcanic events, in *Tidal Phenomena, Lecture Notes in Earth Sciences*, vol. 66, edited by H. Wilheim, W. Zürn, and H. Wenzel, pp. 293–309, Springer-Verlag. 22, 24

Felzer, K. R., and E. E. Brodsky (2005), Testing the stress shadow hypothesis, *J. Geophys. Res.*, *110, B05S09*, doi:10.1029/2004JB003277. 14, 15

Gibbons, J. D. (1985), *Nonparametric Statistical Inference, 2nd ed. revised and expanded*, Marcel Dekker. 15

Gomberg, J., M. L. Blanpied, and N. M. Beeler (1997), Transient triggering of near and distant earthquakes, *Bull. Seismol. Soc. Am.*, *87*, 294–309. 8, 9

Gomberg, J., M. L. Blanpied, N. M. Beeler, and P. Bodin (1998), Earthquake triggering by transient and static deformations, *J. Geophys. Res.*, *103*, 24,411–24,426. 8, 22

Gomberg, J., P. A. Reasenberg, P. Bodin, and R. A. Harris (2001), Earthquakes triggering by seismic waves following the landers and hector mine earthquakes, *Nature*, *411*, 462–466. 14, 21, 22

Habermann, R. E. (1981), Precursory seismicity patterns: stalking the mature seismic cap, in *Earthquake Prediction: an International Review*, edited by D. Simpson and P. Richards, pp. 29–42, American Geophysical Union. 14

Hainzl, S., B. Enescu, M. Cocco, J. Woessner, F. Catalli, R. Wang, and F. Roth (2009), Aftershock modeling based on uncertain stress calculations, *J. Geophys. Res.*, *114*, doi:10.1029/2008JB006011. 23

Harrington, R. M., and E. E. Brodsky (2006), The absence of remotely triggered seismicity in Japan, *Bull. Seismol. Soc. Am.*, *96*, 871–878. 14

Harris, R. A. (1998), Introduction to special section: Stress transfer, earthquake triggering, and time-dependent seismic hazard, *J. Geophys. Res.*, *103*, 24,347–24,358. 24

Heaton, T. H. (1982), Tidal triggering of earthquakes, *Bull. Seismol. Soc. Am.*, *72*, 2180–2200. 3, 23

Hill, D. P., and S. G. Prejean (2009), Dynamic triggering, in *Earthquake Seismology*, edited by H. Kanamori, pp. 257–291, Elsevier. 4, 24

Hill, D. P., P. A. Reasenberg, A. Michael, W. J. Arabaz, G. Beroza, D. Brumbaugh, J. N. Brune, R. Castro, S. Davis, D. dePolo, W. L. Ellsworth, J. Gomberg, S. Harmsen, L. House, S. M. Jackson, M. J. S. Johnston, L. Jones, R. Keller, S. Malone, L. Munguia, S. Nava, J. C. Pechmann, A. Sanford, R. W. Simpson, R. B. Smith, M. Stark, M. Stickney, A. Vidal, S. Walter, V. Wong, and J. Zollweg (1993), Seismicity remotely triggered by the magnitude 7.3 Landers, California, earthquake, *Science*, *260*(5114), 1617–1623. 4, 22

Hill, D. P., F. Pollitz, and C. Newhall (2002), Earthquake-volcano interactions, *Physics Today*, *55 (11)*, 41–47. 22

Ide, S., and G. C. Beroza (2001), Does apparent stress vary with earthquake size?, *Geophys. Res. Lett.*, *28*, 3349–3352. 3

Iwata, T. (2002), Tidal stress/strain and acoustic emission activity at the Uunderground Research Laboratory, canada, *Geophys. Res. Lett.*, *29*, doi:10.1029/2001GL014277. 3

Iwata, T., and H. Katao (2006), Correlation between the phase of the moon and the occurrences of microearthquakes in the Tamba region through point-process modeling, *Geophys. Res. Lett.*, *33*, doi:10.1029/2005GL025510. 17, 20

Iwata, T., and I. Nakanishi (1998), Correlation between earth tide and occurrences of earthquakes in Matsushiro area, Nagano, Japan, *Zisin (J. of Seismol. Soc. of Japan)*, *51*, 51–59. 3

Iwata, T., and I. Nakanishi (2004), Hastening of occurrence of earthquakes due to dynamic triggering: The observation at Matsushiro, central japan, *J. Seismology*, *8*, 165–177. 15

Kanamori, H., and E. Brodsky (2004), The physics of earthquakes, *Reports in Progress in Physics*, *67*, 1429–1496. 6

Kilb, D. (2003), A strong correlation between induced peak dynamic Coulomb stress change from the 1992 M7.3 Landers, California, earthquake and the hypocenter of the 1999 M7.1 Hector mine, California, earthquake, *J. Geophys. Res.*, *108*, doi:10.1029/2001JB000678. 21

Kilb, D., J. Gomberg, and P. Bodin (2000), Triggering of earthquake aftershocks by dynamic stress, *Nature*, *408*, 570–574. 14

Kilb, D., J. Gomberg, and P. Bodin (2002), Aftershock triggering by complete coulomb stress changes, *J. Geophys. Res.*, *107*, doi:10.1029/2001JB000202. 21

Klein, F. W. (1976), Earthquake swarms and the semidurnal solid earth tide, *Geophys. J. Roy. astr. Soc.*, *45*, 245–295. 3

Linde, A. T., I. S. Sacks, M. J. S. Johnston, D. P. Hill, and R. G. Bilham (1994), Increased pressure from rising bubbles as a mechanism for remotely triggered seismicity, *Nature*, *371*, 408–410. 22

Marsan, D., and S. S. Nalbant (2005), Methods for measuring seismicity rate changes: A review and a study of how the m_w 7.3 landers earthquake affected the aftershock sequence of the m_w 6.1 joshua tree earthquake, *Pure Appl. Geophys.*, *162*, 1151–1185. 14

Matsumoto, K., T. Sato, T. Takanezawa, and M. Ooe (2000), Ocean tide models developed by assimimatling TOPEX/POSEIDON altimeter data into hydrodynamical model: A global and a regional model around japan, *J. Oceanogr.*, *56*, 567–581. 23

Matthews, M. V., and P. A. Reasenberg (1988), Statistical methods for investigating quiescence and other temporal seismicity patterns, *Pure Appl. Geophys.*, *126*, 357–372. 14

Métivier, L., O. de Viron, C. P. Conrad, S. Renault, M. Diament, and G. Patau (2009), Evidence of earthquake triggering by the solid earth tides, *Earth Planet. Sci. Lett.*, *278*, 370–375. 3

Miyazawa, M., and J. Mori (2006), Evidence suggesting fluid flow beneath japan due to periodic seismic triggering from the 2004 sumatra-andaman earthquake, *Geophys. Res. Lett.*, *33*, doi:10.1029/2005GL025087. 22

Mohler, A. S. (1980), Earthquake/earth tide correlation and other features of the Susanville, California, earthquake sequence of June-July 1976, *Bull. Seismol. Soc. Am.*, *70*, 1583–1593. 3

Nakanishi, I. (2005), Calculation of theoretical strain seismograms by normal mode theory and computation with observed data from a large deep earthquake, *Geophysical Bulletin of Hokkaido University, Sapporo, Japan*, *68*, 261–269. 23

Nakata, R., N. Suda, and H. Tsuruoka (2008), Non-volcanic tremor resulting from the combined effect of Earth tides and slow slip events, *Nature Geoscience*, *1*, 676–678. 3, 19

Obara, K. (2002), Nonvolcanic deep tremor associated with subduction in southwest japan, *Science*, *296*, 1679–1681. 3

Ogata, Y. (1983), Likelihood analysis of point processes and its applications to seismological data, *Bull. Int. Stat. Inst.*, *50*(Book 2), 943–961. 12, 13

Ogata, Y. (1988), Statistical models for earthquake occurrence and residual analysis for point processes, *J. Am. Stat. Assoc.*, *83*, 9–27. 13

Ogata, Y. (1998), Space-time point-process models for earthquake occurrences, *Ann. Inst. Stat. Math.*, *5*(2), 379–402. 18

Ogata, Y., and H. Akaike (1982), On linear intensity models for mixed doubly stochastic poisson and self-exciting point processes, *J. R. Statist. Soc., Ser. B*, *44*, 102–107. 13

Prejean, S. G., D. P. Hill, E. E. Brodsky, S. E. Hough, M. J. S. Johnston, S. D. Malone, D. H. Oppenheimer, A. M. Pitt, and K. B. Richards-Dinger (2004), Remotely triggered seismicity on the united states west coast following the m_w 7.9 denali fault earthquake, *Bull. Seismol. Soc. Am.*, *94*, S348–S359. 22

Reasenberg, P. A., and M. V. Matthews (1988), Precursory seismic quiescence: A preliminary assesment of the hypothesis, *Pure Appl. Geophys.*, *126*, 373–406. 14

Reasenberg, P. A., and R. W. Simpson (1992), Response of regional seismicity to the static stress change produced by the Loma Prieta earthquake, *Science*, *255*, 1687–1689. 14

Richards-Dinger, K., R. S. Stein, and S. Toda (2010), Decay of aftershock density with distance does not indicate triggering by dynamic stress, *Nature*, *467*, 583–586. 23

Ruina, A. (1983), Slip instability and state variable friction laws, *J. Geophys. Res.*, *88*, 10,359–10,370. 6

Rydelek, P. A., P. M. Davis, and R. Y. Koyanagi (1988), Tidal triggering of earthquake swarms at kilauea volcano, hawaii, *J. Geophys. Res.*, *93*, 4401–4411. 3

Rydelek, P. A., I. S. Sacks, and R. Scarpa (1992), On tidal triggering of earthquakes at Campi Flegrei, Italy, *Geophys. J. Int.*, *109*, 125–135. 3

Savage, J. C., and R. O. Burford (1973), Geodetic determination of relative plate motion in central California, *J. Geophys. Res.*, *78*, 832–845. 8

Schuster, Y. (1897), On lunar and solar periodicities of earthquakes, *Proc. R. Soc. London.*, *61*, 455–465. 11

Schwiderski, E. W. (1980), On charting global ocean tides, *REVIEWS OF GEOPHYSICS*, *18*, 243–268. 23

Souriau, M., A. Souriau, and J. Gagnepain (1982), Modeling and detecting interactions between earth tides and eartquakes with application ro an aftershock sequence in the Pyrenees, *Bull. Seismol. Soc. Am.*, *72*, 165–180. 3

Steacy, S., J. Gomberg, and C. M. (2005), Introduction to special section: Stress transfer, earthquake triggering, and time-dependent seismic hazard, *J. Geophys. Res.*, *110*. 24

Stroup, D. F., D. R. Bohnenstiehl, M. Tolstoy, F. Waldhauser, and R. T. Weekly (2007), Pulse of the seafloor: Tidal triggering of microearthquakes at $9°\,50'$ n east pacific rise, *Geophys. Res. Lett.*, *34*, doi:10.1029/2007GL030088. 3

Tanaka, S. (2010), Tidal triggering of earthquakes precursory to the recent Sumatra megathrust earthquakes of 26 December 2004 (m_w 9.0), 28 March 2005 (m_w 8.6), and 12 September 2007 (m_w 8.5), *Geophys. Res. Lett.*, *37*, doi:10.1029/2009GL041581. 4

Tanaka, S., M. Ohtake, and H. Sato (2002a), Evidence for tidal triggering of earthquakes as revealed from statistical analysis of global data, *J. Geophys. Res.*, *107*, doi:10.1029/2001JB001577. 3, 12, 15, 16, 23

Tanaka, S., M. Ohtake, and H. Sato (2002b), Spatio-temporal variation of the tidal triggering effect on earthquake occurrence associated with the 1982 South Tonga earthquake of mw 7.5, *Geophys. Res. Lett.*, *29*, doi:10.1029/ 2002GL015386. 4, 15, 16, 17

Thatcher, W. (1979), Systematic inversion of geodetic data in central California, *J. Geophys. Res.*, *84*, 2283–2295. 8

Thomas, A. M., R. M. Nadeau, and R. Bürgmann (2009), Tremor-tide correlations and near-lithostatic pore pressure on the deep san andreas fault, *Nature*, *462*, 1048–1051. 3

Toda, S., R. S. Stein, P. A. Reasenberg, J. M. Dieterich, and A. Yoshida (1998), Stress transferred by the 1995 $m_w = 6.9$ kobe, japan, shock: Effect on aftershocks and future earthquake probabilities, *J. Geophys. Res.*, *103*, 24,543–24,565. 19

Tolstoy, M., F. L. Vernon, J. A. Orcutt, and E. K. Wyatt (2002), Breathing of the seafloor: tidal correlations of seismicity at axial volcano, *Geology*, *30*, 503–506. 3

Tsuruoka, H., M. Ohtake, and H. Sato (1995), Statistical test of the tidal triggering of earthquakes: Controbution of the ocean tide loading effect, *Geophys. J. Int.*, *122*, 183–194. 3, 5, 15, 23

van der Elst, N. J., and E. E. Brodsky (2010), Connecting near-field and far-field earthquake triggering to dynamic strain, *J. Geophys. Res.*, *115*, doi:10.1029/2009JB006681. 15

Vidale, J. E., D. C. Agnew, M. J. S. Johnston, and D. H. Oppenheimer (1998), Absence of earthquake correlation with Earth tides: An indication of high preseismic fault stress rate, *J. Geophys. Res.*, *103*, 24,567–24,572. 3

West, M., J. J. Sanchez, and S. R. McNutt (2005), Periodically triggered seismicity at Mount Wrangell, Alaska, after the Sumatra earthquake, *Science*, *308*, 1144–1146. 22

Wilcock, W. S. D. (2001), Tidal triggering of microearthquakes on the Juan de Fuca Ridge, *Geophys. Res. Lett.*, *28*, 3999–4002. 3

Wilcock, W. S. D. (2009), Tidal triggering of earthquakes in the Northeast Pacific Ocean, *Geophys. J. Int.*, *179*, 1055–1070. 3

Yin, X. C., X. Z. Chen, Z. P. Song, and C. Yin (1995), A new approach to earthquake prediction: The Load/Unload Response Ratio (LURR) theory, *Pure Appl. Geophys.*, *145*, 701–715. 4

Yin, X. C., Y. C. Wang, K. Y. Peng, Y. L. Bai, H. T. Wang, and X. F. Yin (2000), Development of a new approach to earthquake prediction: The load/unload response ratio (LURR) theory, *Pure Appl. Geophys.*, *157*, 2365–2383. 4

Zhang, Y., X. Yin, K. Peng, H. Wang, J. Zheng, Y. Wu, and L. Zhang (2006), LURR and the San Simeon M 6.5 earthquake in 2003 and the seismic tendency in CA, *Pure Appl. Geophys.*, *163*, 2343–2351. 4